Electroreduction of Chlorine Gas at Platinum Electrodes in Several Room Temperature Ionic Liquids: Evidence of Strong Adsorption on the Electrode Surface Revealed by Unusual Voltam…

ARTICLE *in* THE JOURNAL OF PHYSICAL CHEMISTRY C · DECEMBER 2008

Impact Factor: 4.77 · DOI: 10.1021/jp8082437

6 AUTHORS, INCLUDING:

Debbie S. Silvester
Curtin University
55 PUBLICATIONS **1,684** CITATIONS
SEE PROFILE

Leigh Aldous
University of New South Wales
89 PUBLICATIONS **1,836** CITATIONS
SEE PROFILE

Electroreduction of Chlorine Gas at Platinum Electrodes in Several Room Temperature Ionic Liquids: Evidence of Strong Adsorption on the Electrode Surface Revealed by Unusual Voltammetry in Which Currents Decrease with Increasing Voltage Scan Rates

Xing-Jiu Huang,[†] Debbie S. Silvester,[†] Ian Streeter,[†] Leigh Aldous,[‡] Christopher Hardacre,[‡] and Richard G. Compton*,[†]

Department of Chemistry, Physical and Theoretical Chemistry Laboratory, Oxford University, South Parks Road, Oxford OX1 3QZ, United Kingdom, and School of Chemistry and Chemical Engineering/ QUILL, Queen's University Belfast, Belfast, Northern Ireland BT9 5AG, United Kingdom

Received: September 16, 2008; Revised Manuscript Received: October 5, 2008

Voltammetry is reported for chlorine, Cl_2, dissolved in various room temperature ionic liquids using platinum microdisk electrodes. A single reductive voltammetric wave is seen and attributed to the two-electron reduction of chlorine to chloride. Studies of the effect of voltage scan rate reveal uniquely unusual behavior in which the magnitude of the currents decrease with increasing scan rates. A model for this is proposed and shown to indicate the presence of strongly adsorbed species in the electrode reaction mechanism, most likely chlorine atoms, $Cl^{\bullet}_{(ads)}$.

1. Introduction

Room temperature ionic liquids (RTILs) are compounds composed entirely of ions and exist in the liquid state at and around room temperature.[1−4] They are generally comprised of a bulky organic cation and a weakly coordinating inorganic anion. Ideally, they can possess several characteristic properties such as intrinsic conductivity, high thermal stability, high viscosity, high polarity, and wide electrochemical windows. Much research has focused on employing RTILs as media in several applications such as "green" synthesis,[5] catalysis,[6,7] and biochemical applications[8] and in electrochemical devices.[1,3] In particular, RTILs have shown promise for use as electrolytes in Clark-cell type gas sensors.[9] Before employing RTILs as electrolytes in gas sensors, it is important to study the reactions and mechanisms of each target gas in a range of RTIL media to determine the optimum cation/anion combination for each system. Voltammetric and mechanistic studies on the electrochemical reductions and oxidations of several gases, including oxygen,[10] hydrogen,[11,12] ammonia,[13,14] sulfur dioxide,[15] nitrogen dioxide,[16] and hydrogen sulfide,[17] in RTILs have been recently presented. For hydrogen and ammonia oxidation,[11,12,14] it was found that the nature of the RTIL anion in particular had a strong effect on the shape, size, and formal potential of voltammetric waves. In the present paper we look at the electrochemical behavior of chlorine gas[18] in several ionic liquids and discover highly unusual voltammetry.

There are several reports on the electrochemical reduction of chlorine gas in aqueous solutions.[19−22] For example, Lowe et al.[19] studied the voltammetry of chlorine in aqueous solutions on different carbon-based electrodes and found that edge-plane pyrolytic electrodes showed much promise as an electrode material in a Clark-cell type sensor for chlorine detection. Sun et al.[20] report the electrocatalytic reduction of chlorine by multiwalled carbon nanotubes (MWNTs) in sulfuric acid solution and found that the higher accessible surface area of the MWNTs allowed for excellent sensitivity at low concentrations of chlorine. In both cases, the mechanism for chlorine reduction involved participation of protons from the solvent. However, there are very few mechanistic studies for chlorine reduction in aprotic solvents. Sereno et al.[23] report the electrochemical behavior of chlorine in acetonitrile at platinum rotating disk electrodes. They found one reduction wave and one oxidation wave, which were both under diffusion control, and the reduction wave was assigned to the following two-electron process:[23]

$$Cl_2 + 2e^- \rightarrow 2Cl^- \quad (1)$$

Recently, Rogers et al.[24] reported the electrochemistry of iodine (I_2) in the RTIL $[C_4mim][NTf_2]$ (1-butly-3-methylimidazolium bis(trifluoromethylsulfonyl)imide). Two reduction peaks were observed and were assigned to the following equations:[24]

$$3I_2 + 2e^- \rightarrow 2I_3^- \quad (2)$$

$$I_3^- + 2e^- \rightarrow 3I^- \quad (3)$$

The first wave was theoretically simulated over a range of scan rates by splitting eq 2 into two separate steps, involving the generation of iodide as an intermediate species:[24]

$$I_2 + 2e^- \rightarrow 2I^- \quad (4)$$

$$I^- + I_2 \rightarrow I_3^- \quad (5)$$

In this work, we report the electrochemical reduction of chlorine gas in several different RTILs (the structures of the anions and cations employed are shown in Figure 1). A main aim is to investigate the electrochemical mechanism of chlorine reduction in RTILs and compare it to that of iodine reduction. Several RTILs will be employed to determine if the voltammetric behavior is the same when the nature of the cation or anion is changed. In particular, the voltammetry is discovered

* To whom correspondence should be addressed E-mail: richard.compton@chem.ox.ac.uk. Tel.: +44 (0) 1865 275 413. Fax: +44 (0) 1865 275 410.
[†] Oxford University.
[‡] Queen's University Belfast.

10.1021/jp8082437 CCC: $40.75
Published on Web 11/13/2008

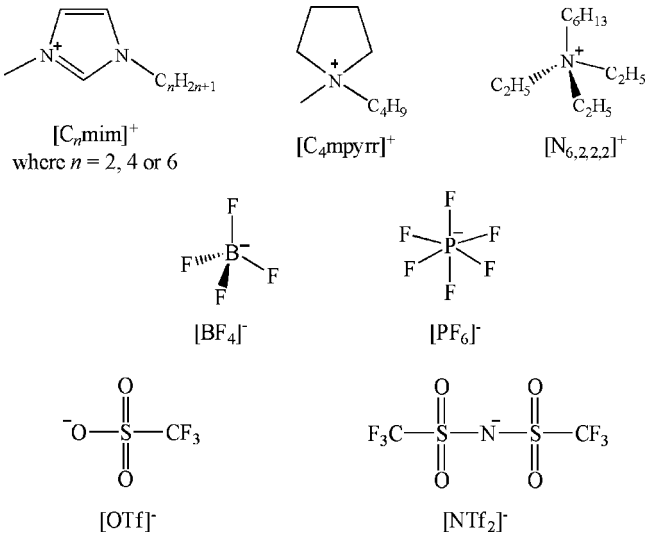

Figure 1. Molecular structures of the anions and cations used as the RTIL solvents in this study.

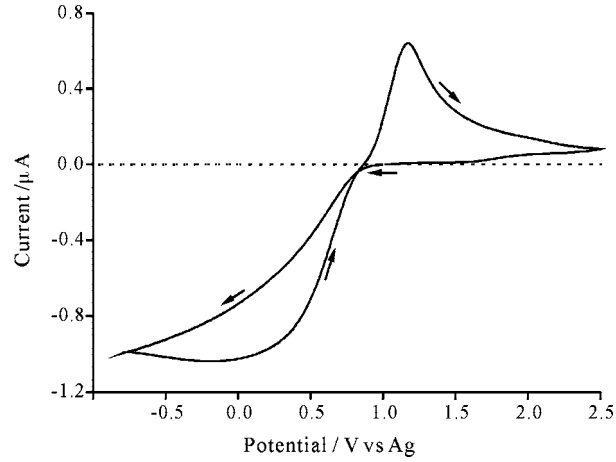

Figure 2. Typical cyclic voltammetry for the reduction of 1 atm Cl_2 gas in [C_4mpyrr][NTf_2] on a 10 μm diameter platinum electrode at a scan rate of 1 V s^{-1}. The dotted line shows a blank sample of [C_4mpyrr][NTf_2] without Cl_2 under the same conditions.

to be highly unusual in the sense that increasing voltage scan rates lead to diminished current signals in stark contrast to what is usually observed for simple diffusion-controlled or surface-confined voltammetry. A model to account for this behavior is proposed.

2. Experimental Section

2.1. Chemical Reagents. *N*-Butyl-*N*-methylpyrrolidinium bis(trifluoromethylsulfonyl)imide ([C_4mpyrr][NTf_2]), 1-ethyl-3-methylimidazolium bis(trifluoromethylsufonyl)imide ([C_2mim][NTf_2]), 1-butyl-3-methylimidazolium bis(trifluoromethylsulfonyl)imide ([C_4mim][NTf_2]), *N*-hexyltriethylammonium bis(trifluoromethylsulfonyl)imide ([$N_{6,2,2,2}$][NTf_2]), and 1-hexyl-3-methylimidazolium chloride ([C_6mim]Cl) were synthesized according to standard literature procedures.[25,26] 1-Butyl-3-methylimidazolium trifluoromethylsulfonate ([C_4mim][OTf]), 1-butyl-3-methylimidazolium tetrafluoroborate ([C_4mim][BF_4]), and 1-butyl-3-methylimidazolium hexafluorophosphate ([C_4mim][PF_6]) were kindly donated by Merck KGaA. [C_4mim][BF_4] and [C_4mim][PF_6] were used as received. [C_4mim][OTf] was first diluted with Ch_2Cl_2 and passed through a column consisting of alternating layers of neutral aluminum oxide and silica gel to remove residual acidic impurities. Ferrocene ($Fe(C_5H_5)_2$, Fc, Aldrich, 98%), tetra-*n*-butylammonium perchlorate (TBAP, Fluka, Puriss electrochemical grade, >99%), and acetronitrile (Fischer Scientific, dried and distilled, >99.99%) were used as received without further purification. Chlorine gas (99.5%) was purchased from ARGO, Basildon, UK.

2.2. Instrumentation. Cyclic voltammetry (CV) was performed using a type-III μ-Autolab (Eco Chemie, Utrecht, Netherlands), which was interfaced with a PC using GPES (version 4.9) software for Windows. Measurements were performed using a two-electrode cell consisting of a platinum microelectrode (10 μm diameter) as the working electrode and a silver wire (0.5 mm diameter) as the quasi-reference electrode. The electrodes were housed in a glass "T-cell" specially designed[11,27] to control the environment of the RTIL. The diameter of the microdisk electrode was calibrated electrochemically using 2 mM ferrocene (+0.1 M TBAP) in acetonitrile, adopting a value for the diffusion coefficient of 2.3×10^{-9} m^2 s^{-1} at 298 K.[28] A disposable micropipette tip was attached to the end of the microdisk electrode to provide a cavity in which 20 μL of blank ionic liquid was placed. Prior to the addition of gases, the T-cell containing the ionic liquid was purged under vacuum (Edwards high-vacuum pump, model ES 50) for at least 90 min until the baseline showed no trace of atmospheric oxygen or moisture. Chlorine gas was introduced via PTFE tubing through one arm of the T-cell, allowed to pass over the RTIL, then flow out through the other arm of the cell. The ionic liquid was reversibly saturated with gas after ca. 30−40 min, as evidenced by maximum stable peak currents. Outgassing of the RTIL after saturation indicated no irreversible chemical changes due to reaction of chlorine with the RTIL.

3. Results and Discussion

Eight room temperature ionic liquids with different cations and anions, namely, [C_4mpyrr][NTf_2], [C_2mim][NTf_2], [C_4mim][NTf_2], [$N_{6,2,2,2}$][NTf_2], [C_4mim][OTf], [C_4mim][BF_4], [C_4mim][PF_6], and [C_6mim]Cl, were chosen as suitable solvents for electrochemical experiments since they all showed no noticeable voltammetric features in the absence of chlorine when fully purged under vacuum.

3.1. Preliminary Observations of Reduction of Chlorine Gas in RTILs. Before cyclic voltammetry is presented for the reduction of chlorine gas in all eight ionic liquids, the voltammetry is first considered in one ionic liquid, namely, [C_4mpyrr][NTf_2]. Figure 2 shows the reduction of 1 atm chlorine gas in [C_4mpyrr][NTf_2] on a 10 μm diameter Pt electrode at a scan rate of 1 V s^{-1}. The potential was swept from a position of zero current (at +1.0 V vs Ag) down to −0.8 V and back up to +2.5 V. As can be observed, a very broad reductive feature is obtained on the reductive cycle, with a relatively high current on such a small microelectrode (cf. 6 nA for 1 atm O_2 in [C_2mim][NTf_2] on the same size electrode). After reversal of the potential at −0.8 V, the current becomes *larger* than that on the forward scan, ultimately resulting in hysteresis and a crossing over of the scans at ca. +0.75 V. A very sharp anodic peak was then observed at ca. +1.2 V, which is directly related to the reduction feature since no such peak was observed when the current was swept positively from +0.9 V to solvent breakdown. This observation also suggests that chlorine cannot be electrochemically oxidized in this system.

The reduction wave can be attributed to a two-electron step, which is analogous to that previously proposed in acetonitrile (eq 1).[23] The appearance of just one reduction wave (in contrast

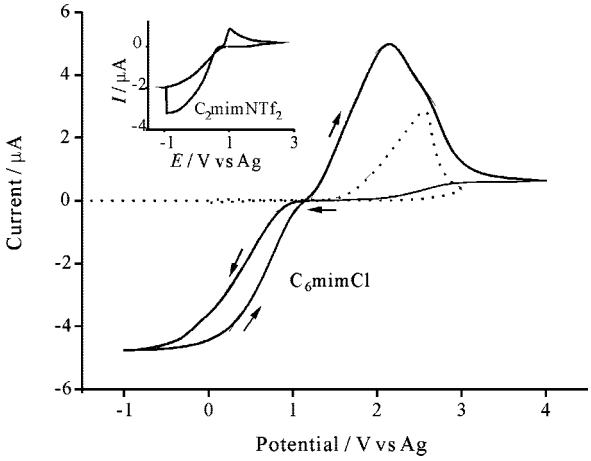

Figure 3. Cyclic voltammetry for the reduction of 1 atm Cl_2 gas in [C_6mim]Cl on a 10 μm diameter platinum electrode at a scan rate of 4 V s^{-1}. The dotted line shows a blank sample of [C_6mim]Cl without Cl_2 under the same conditions. The inset shows the effect of holding the potential for 20 s at −1.0 V in [C_2mim][NTf_2] on a 10 μm diameter platinum electrode at 1 V s^{-1}.

to the two reduction peaks seen for iodine)[24] suggests that the follow-up chemical step observed for iodine (eq 5) does not take place for chlorine in ionic liquids. This might explain why a second reductive feature is not observed for chlorine in Figure 2 (no additional features were seen after the potential is swept to solvent breakdown).

The current was also observed to increase when the potential is swept past the reduction peak and "held" for 20 s at −1.0 V in [C_2mim][NTf_2] (see Figure 2 inset). As can be seen, the current increases from ca. −2 to −3.5 μA when the potential is held, suggesting that the electrode is being "unblocked". The same behavior was observed in all RTILs studied, but the voltammetry is not shown.

Based on the mechanism proposed (eq 1), it is believed that the resulting oxidative back peak at +1.2 V is due to the oxidation of chloride, which could be either "bulk" (i.e., diffusional) or "adsorbed" on the surface. To suggest if the peak is bulk or adsorbed chloride, the oxidation of chlorine gas was studied in a chloride-based ionic liquid (providing free bulk chloride ions). Figure 3 (solid line) shows the reduction of chlorine gas in [C_6mim]Cl on a 10 μm diameter Pt electrode at a scan rate of 4 V s^{-1}. The voltammetric behavior is similar to that observed in [C_4mpyrr][NTf_2] (Figure 2). However, an extra oxidative peak (or shoulder) is seen at ca. +2.6 V vs Ag, which overlays well with the oxidation of chloride from a blank sample of [C_6mim]Cl (dotted line). This suggests that the oxidative peak seen after the reduction of chlorine is most likely due to the oxidation of adsorbed (not bulk) chloride. We now consider the reduction of chlorine in a range of RTILs.

3.2. Reduction of Chlorine Gas in Different RTILs. Several different RTILs were chosen as solvents in which to study the reduction of chlorine gas since it has previously been shown that changing the nature of the cation and anion had a strong effect on the size and shape of the voltammetry for hydrogen[11,12] oxidation in RTILs. The voltammograms for H_2S[17] and SO_2[15] reduction, however, were approximately the same when the RTIL was changed, but the attainable limiting currents were found to vary between each solvent.

Figure 4 shows the reduction of 1 atm Cl_2 gas on a 10 μm diameter Pt electrode at a range of scan rates in four RTILs with a common $[NTf_2]^-$ anion. In all four RTILs, the voltammetry is approximately similar, with one broad reduction feature, and a sharper oxidative feature on the reverse sweep at ca. +1 to 1.5 V vs Ag. The limiting currents are similar in all four RTILs, suggesting that the nature of the cation does not have a significant effect on the voltammetric behavior.

The nature of the anion was also varied. Figure 5 shows the reduction of 1 atm Cl_2 gas on a 10 μm diameter Pt electrode at a range of scan rates in four imidazolium ($[C_n\text{mim}]^+$) RTILs with different anions. Again, the voltammetry is not very different from that presented in Figure 4, suggesting that the nature of the anion also does not have an influence on the voltammetric behavior.

The scan rate dependence on the peak currents of the voltammograms presented in Figures 4 and 5 is highly unusual. As the scan rate is increased, the peak current for the reduction peak *decreases*; this behavior is rarely observed experimentally. Plots of peak current (reduction and oxidation) against both (a) scan rate and (b) square root of scan rate are presented in Figure 6 in one chosen RTIL ([C_4mpyrr][NTf_2]). Similar behavior was observed in all other RTILs studied. We address this behavior in section 4 below.

In our previous studies on gases (H_2, NH_3, O_2, SO_2, and H_2S)[10−15,17] in RTILs, potential step chronoamperometry is often used to obtain diffusion coefficients and solubilities of the gas in each RTIL. However, the nature of the voltammetry of chlorine on the Pt electrode surface makes the experimental transient impossible to fit to the Shoup and Szabo expression,[29] which is only sufficient to describe a simple *n*-electron transfer. It is believed that the diffusion coefficients of Cl_2 in all eight RTILs should be of the approximate order 10^{-10} m^2 s^{-1}, the same order of magnitude as that found for most gaseous species in RTILs. The limiting currents shown in Figures 4 and 5 are very high compared to, for example, that of oxygen (cf. 6 nA for 1 atm O_2 in [C_2mim][NTf_2] on the same size electrode),[10] suggesting that the concentration (or solubility) of chlorine is very high in RTILs. In particular, the highest limiting currents were seen in [C_6mim]Cl (Figure 5d), suggesting that Cl_2 may have a very strong interaction with the chloride ionic liquid.

3.3. Reduction of Chlorine Gas in Acetonitrile. To compare the electrochemical behavior of Cl_2 in RTILs to that in a conventional molecular solvent, the reduction of chlorine was also studied in acetonitrile. Figure 7 shows the reduction of 1 atm chlorine gas on a 10 μm diameter Pt electrode at a range of scan rates in acetonitrile (+0.1 M TBAP). The potential was swept from +1.0 to −0.5 V (where the scan is reversed) and then up to +1.5 V. The onset of chlorine gas reduction begins at ca. +0.8 V, after which the current steadily increases at more negative potentials. When the scan is reversed at −0.5 V, the reverse sweep records a higher current than the forward scan, analogous to that observed in RTILs (see Figure 2). The reduction currents are similar to those seen in the eight RTIL solvents studied (Figures 4 and 5), despite the much higher viscosity (and hence lower expected currents) of the RTILs compared to those of MeCN. This suggests that chlorine gas may be more soluble in RTILs than in MeCN, which may be highly advantageous if employing RTILs as electrolytes in chlorine gas sensors.

In contrast to the behavior seen in all eight RTILs studied, the peak currents increase with increasing scan rate, typical of almost all diffusional or adsorbed species. Sereno et al.[23] reported that the reduction peak appeared to be diffusion-controlled in MeCN since a linear relationship was observed between the limiting current and the square root of the rotation speed of the macroelectrode. A plot of the (approximate) reduction peak current against the square root of scan rate in

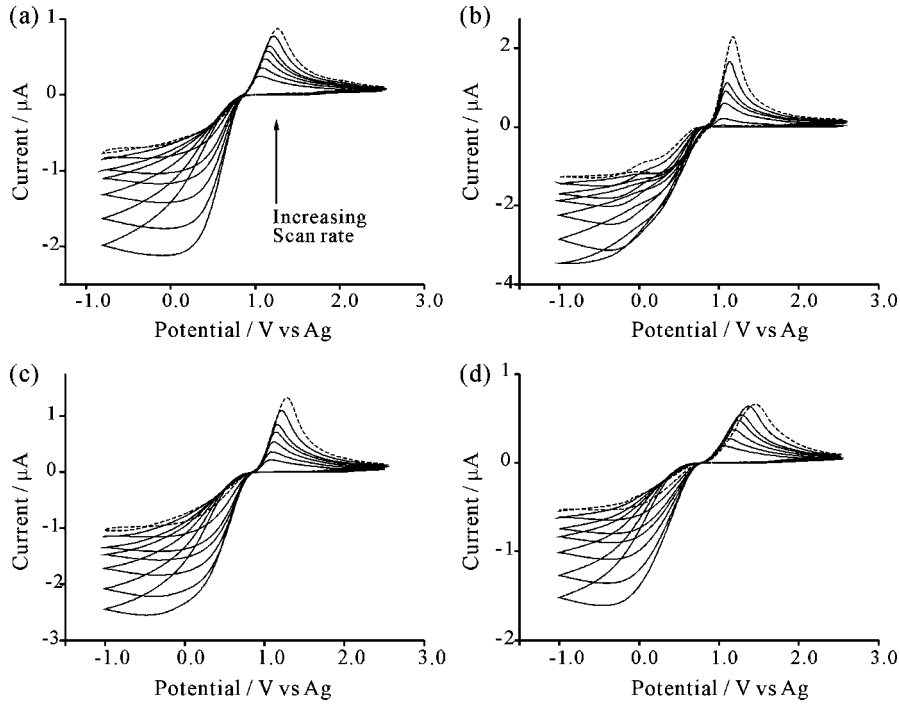

Figure 4. Typical cyclic voltammograms at a range of scan rates (0.1, 0.2, 0.4, 0.7, 1, 2, and 4 V s^{-1}) for the reduction of 1 atm Cl_2 on a 10 μm diameter platinum electrode in (a) [C_4mpyrr][NTf_2], (b) [C_2mim][NTf_2], (c) [C_4mim][NTf_2], and (d) [N_{6222}] [NTf_2]. The dotted lines correspond to a scan rate of 4 V s^{-1}.

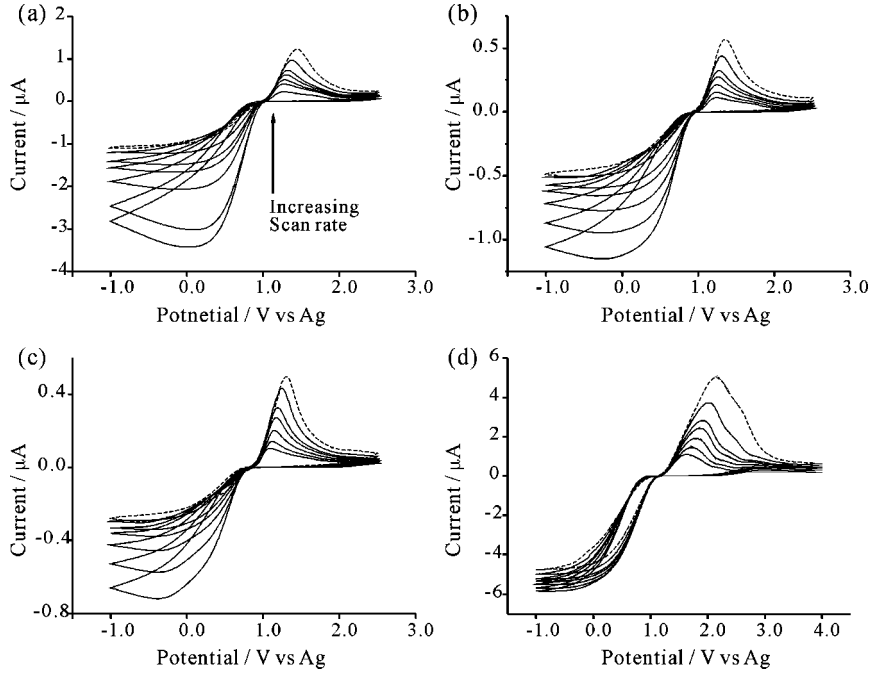

Figure 5. Typical cyclic voltammograms at a range of scan rates (0.1, 0.2, 0.4, 0.7, 1, 2, and 4 V s^{-1}) for the reduction of 1 atm Cl_2 on a 10 μm diameter platinum electrode in (a) [C_4mim][OTf], (b) [C_4mim][BF_4], (c) [C_4mim][PF_6], and (d) [C_6mim]Cl. The dotted lines correspond to a scan rate of 4 V s^{-1}.

this work is shown in Figure 7a. The near scan rate independence suggests that a fast diffusion rate to the microelectrode leads to near steady-state behavior.

As seen for the reduction of chlorine in all RTILs studied, there is also a small oxidative "back" peak in acetonitrile (Figure 7 at +1.2 V), which increases with increasing scan rate (opposite to that observed in RTILs). A plot of peak current vs the square root of scan rate for the oxidation peak in MeCN is shown in Figure 8b. A linear relationship is observed between current and the square root of scan rate, suggesting that the oxidation process is diffusion-controlled. This is consistent with that reported by Sereno et al.[23] for chlorine reduction in MeCN.

4. Theoretical Model and Numerical Simulation

4.1. Simulation Details. Numerical simulations are presented in this section to illustrate how the adsorption of chlorine onto the electrode surface can lead to the voltammetry observed in the experiments. The adsorption of Cl_2 can be a nondissociative process, as described by the following reaction step:

$$Cl_{2(soln)} \underset{k_b}{\overset{k_f}{\rightleftharpoons}} Cl_{2(ads)} \quad (6)$$

Alternatively, chlorine can adsorb in a dissociative manner to form chlorine atoms on the electrode surface:

$$Cl_{2(soln)} \underset{k_b}{\overset{k_f}{\rightleftharpoons}} 2Cl^{\bullet}_{(ads)} \quad (7)$$

The amount of adsorbed species on the electrode is quantified by the parameter θ, which is the fraction of surface sites that

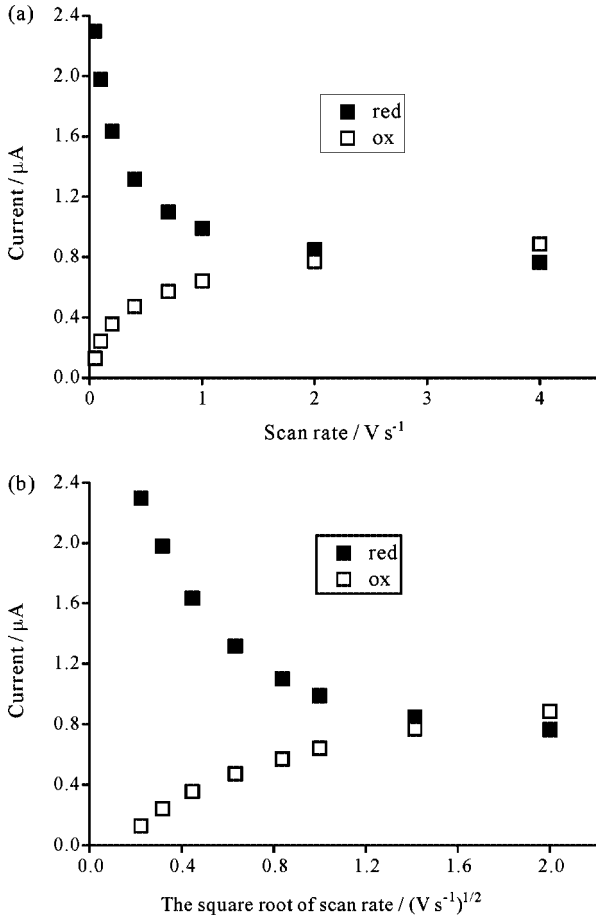

Figure 6. Plots of the reduction peak current of Cl_2 and oxidation peak current of Cl^- in $[C_4mpyrr][NTf_2]$ (Figure 2) against (a) the scan rate and (b) the square root of the scan rate.

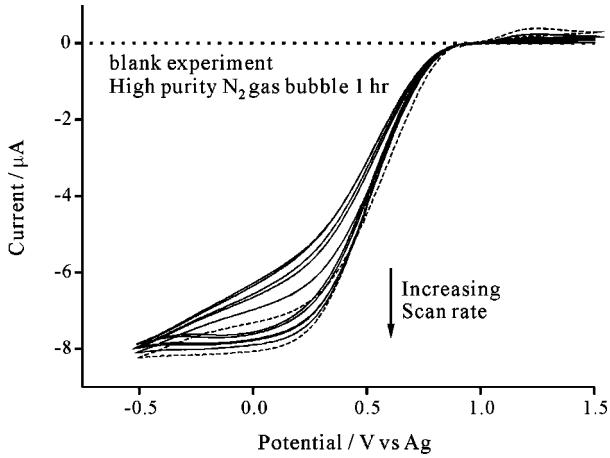

Figure 7. Cyclic voltammograms of the reduction of 1 atm Cl_2 in MeCN (+0.1 M TBAP) on a 10 μm diameter platinum electrode at a range of scan rates from 0.1 to 4 V s^{-1}. The dotted line corresponds to the same solution in the absence of Cl_2 under the same conditions.

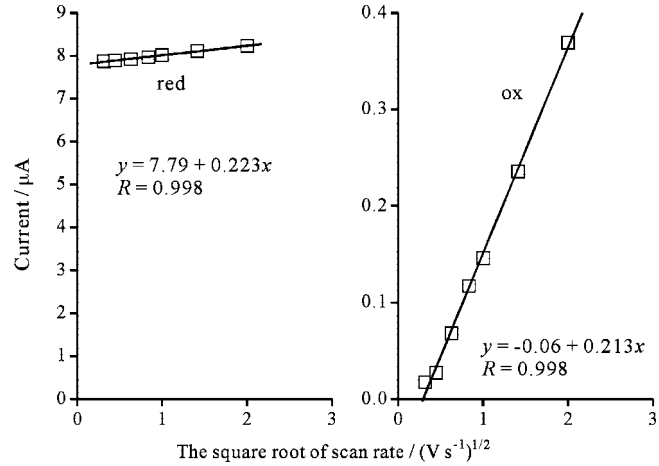

Figure 8. Plots of (a) the reduction peak current of Cl_2 and (b) oxidation peak current of Cl^- against the square root of the scan rate in MeCN (+0.1 M TBAP) as shown in Figure 7.

are occupied. The rate of the nondissociative adsorption is given by the following expression:

$$\frac{\partial\theta}{\partial t} = k_f(1-\theta)[Cl_2] - k_b\theta \quad (8)$$

The corresponding expression for the dissociative process is second order with respect to the surface coverage:

$$\frac{\partial\theta}{\partial t} = k_f(1-\theta)^2[Cl_2] - k_b\theta^2 \quad (9)$$

In the numerical simulations described here, it is assumed that the reduction of chlorine can only occur on unoccupied electrode sites. Large values of θ therefore reduce the effective surface area that is available for the electron transfer and reduce the magnitude of the faradaic current.

The following electron transfer reaction takes place at the electrode surface:

$$Cl_2 + e^- \rightleftarrows 2Cl^- \quad (10)$$

The numerical methods for simulating such an electron transfer reaction at a microdisk has been described in detail in our previous paper on the reduction of iodine.[24] The mass transport of both species Cl_2 and Cl^- in solution is given by Fick's second law of diffusion:

$$\frac{\partial C}{\partial t} = D\left(\frac{\partial^2 C}{\partial z^2} + \frac{\partial^2 C}{\partial r^2} + \frac{1}{r}\frac{\partial C}{\partial r}\right) \quad (11)$$

where z and r are the cylindrical radial coordinates, D is the diffusion coefficient, and C is the concentration. At the start of the potential sweep simulation, the concentration of Cl_2 is set equal to its bulk solution value and the concentration of Cl^- is set equal to zero at all points in solution. The starting fractional surface coverage is set so that the processes of adsorption and desorption are in equilibrium. A condition of zero diffusional flux is applied as a boundary condition at the disk's axis of symmetry and at the insulating surface surrounding the disk. Concentrations are set equal to their bulk solution values at a distance $6\sqrt{Dt}$ from the electrode surface, beyond which the electron-transfer reaction has no influence.[30] The boundary condition at the electrode is the Butler−Volmer rate equation for the electron transfer:

$$D\frac{\partial[Cl_2]}{\partial z} = k_a \exp\left(\frac{-\alpha F}{RT}(E - E_a^0)\right)[Cl_2] - k_b \exp\left(\frac{\beta F}{RT}(E - E_b^0)\right)[Cl^-] \quad (12)$$

where k_a and k_b are rate constants, E_a^0 and E_b^0 are formal electrode potentials, and α and β are charge-transfer coefficients. Equation 12 can be rewritten as eq 13, which uses the alternative heterogeneous rate constants k_a' and k_b' and does not contain the formal electrode potentials:

$$D\frac{\partial[Cl_2]}{\partial z} = k_a' \exp\left(\frac{-\alpha F}{RT}E\right)[Cl_2] - k_b' \exp\left(\frac{\beta F}{RT}E\right)[Cl^-] \quad (13)$$

This is the analogue of the expression that was successfully used for simulating the reduction of iodine.[24] A further boundary condition at the electrode requires that the flux of the two species at the electrode surface are equal in magnitude:

$$D_{Cl_2}\frac{\partial[Cl_2]}{\partial z} = -D_{Cl^-}\frac{\partial[Cl^-]}{\partial z} \quad (14)$$

Implicit in the above model is the assumption that chloride formation does not lead to phase separation.

The mass-transport equations and the corresponding boundary conditions were solved using the alternating direction implicit finite difference scheme in conjunction with the Thomas algorithm to generate concentration profiles of the two species. It should be noted that the concentration of Cl_2 varies across the surface of the nonuniformly accessible electrode, and therefore the value of θ is also nonuniform across the surface. The value of θ was calculated at each discretized node on the electrode surface and at each time step using either eq 8 or eq 9. The current at the microdisk is found from the concentration gradient at the electrode surface, and it is also scaled by the fraction of the electrode surface that is available for the electron transfer, $(1 - \theta)$:

$$i = -4\pi FD\int_0^{r_d} \frac{\partial[Cl_2]}{\partial z}(1-\theta)r\,dr \quad (15)$$

The simulation grid used was that described by Gavaghan, which uses a fine mesh density near the singularity at the edge of the disk electrode.[31] The simulation program was tested for convergence by ensuring that an increase in the number of spatial or temporal nodes lead to a negligible change in the simulated current.

4.2. Simulated Voltammetry. Figure 9 shows simulated voltammetry at three different scan rates. The simulations used diffusion coefficients of 10^{-6} and 4×10^{-7} cm^2 s^{-1} for Cl_2 and Cl^-, respectively, which are typical values for small molecules in RTILs near 25 °C. The values $k_a' = 100$ cm s^{-1} and $k_b' = 10^{-12}$ cm s^{-1} were used for the heterogeneous rate constants in eq 13, and the charge-transfer coefficients were both equal to 0.5. The adsorption of Cl_2 was assumed to be nondissociative, and the values $k_f = 50$ mol^{-1} cm^3 s^{-1} and $k_b = 0.1$ s^{-1} were used for the rate constants in eq 8. The starting concentration of dissolved Cl_2 was 6 M. Note that these values have been chosen for illustrative purposes; we do not claim to have "fitted" the experimental and simulated voltammetry.

The simulated voltammetry in Figure 9 is qualitatively similar to the experimental voltammetry in Figure 5a for the reduction of chlorine in $[C_4mpyrr][NTf_2]$. The cathodic current continues to increase in magnitude after the potential sweep has changed direction at −0.8 V. As Cl_2 is consumed at the electrode by the electron-transfer reaction, the equilibrium for adsorption in eq 6 becomes unbalanced, and there is a net desorption of Cl_2. This makes more of the electrode surface available for the electron-transfer reaction, and so the current increases as time progresses. Furthermore, the cathodic current increases in magnitude with decreasing scan rate, as was seen with the experimental voltammetry. This occurs because there is more significant desorption of Cl_2 from the electrode surface for the longer time scale experiments. Qualitatively similar voltammetry was also obtained when the adsorption of Cl_2 was assumed to be dissociative and eq 9 was used instead of eq 8.

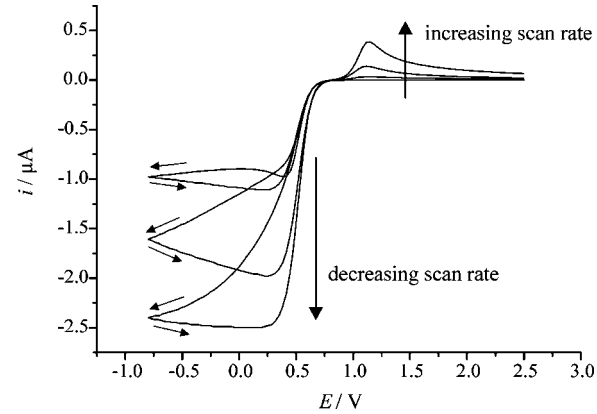

Figure 9. Simulated voltammetry using scan rates 0.05, 0.2, and 1 V s^{-1} and the parameters given in section 4.2. The unlabeled arrows indicate the direction of the potential sweep.

5. Conclusions

The adsorption model presented above suggests that the reduction of chlorine in RTIL solvents involves a strongly adsorbed and kinetically significant intermediate. It is very likely that this is $Cl^{\bullet}_{(ads)}$ on the basis of diverse observations on the Cl_2/Pt system[23,32−34] but other possibilities cannot be absolutely discounted on the basis of voltammetry alone. The large voltammetric currents measured indicate that Cl_2 has a high solubility in RTILs, typically in the range 1−10 M. This makes these solvents attractive for the purposes of gas sensors.

Acknowledgment. We thank the EPSRC for financial support for X.-J.H. and a studentship for I.S. D.S.S. thanks Schlumberger (Cambridge), UK, for support.

References and Notes

(1) Buzzeo, M. C.; Evans, R. G.; Compton, R. G. *ChemPhysChem* **2004**, *5*, 1106.
(2) Marsh, K. N.; Deev, A.; Wu, A. C. T.; Tran, E.; Klamt, A. *Kor. J. Chem. Eng.* **2002**, *19*, 357.
(3) Silvester, D. S.; Compton, R. G. *Z. Phys. Chem.-Int. J. Res. Phys. Chem. Chem. Phys.* **2006**, *220*, 1247.
(4) Endres, F.; El Abedin, S. Z. *Phys. Chem. Chem. Phys.* **2006**, *8*, 2101.
(5) Earle, M. J.; Seddon, K. R. *Pure Appl. Chem.* **2000**, *72*, 1391.
(6) Wasserscheid, P.; Keim, W. *Angew. Chem., Int. Ed.* **2000**, *39*, 3773.
(7) Parvulescu, V. I.; Hardacre, C. *Chem. Rev.* **2007**, *107*, 2615.
(8) van Rantwijk, F.; Sheldon, R. A. *Chem. Rev.* **2007**, *107*, 2757.
(9) Buzzeo, M. C.; Hardacre, C.; Compton, R. G. *Anal. Chem.* **2004**, *76*, 4583.
(10) Buzzeo, M. C.; Klymenko, O. V.; Wadhawan, J. D.; Hardacre, C.; Seddon, K. R.; Compton, R. G. *J. Phys. Chem. A* **2003**, *107*, 8872.
(11) Silvester, D. S.; Aldous, L.; Hardacre, C.; Compton, R. G. *J. Phys. Chem. B* **2007**, *111*, 5000.
(12) Silvester, D. S.; Ward, K. R.; Aldous, L.; Hardacre, C.; Compton, R. G. *J. Electroanal. Chem.* **2008**, *618*, 53.
(13) Buzzeo, M. C.; Giovanelli, D.; Lawrence, N. S.; Hardacre, C.; Seddon, K. R.; Compton, R. G. *Electroanalysis* **2004**, *16*, 888.

(14) Ji, X. B.; Silvester, D. S.; Aldous, L.; Hardacre, C.; Compton, R. G. *J. Phys. Chem. C* **2007**, *111*, 9562.
(15) Silvester, D. S.; Rogers, E. I.; Barrosse-Antle, L. E.; Broder, T. L.; Compton, R. G. *J. Braz. Chem. Soc.* **2008**, *19*, 611.
(16) Broder, T. L.; Silvester, D. S.; Aldous, L.; Hardacre, C.; Compton, R. G. *J. Phys. Chem. B* **2007**, *111*, 7778.
(17) O'Mahony, A. M.; Silvester, D. S.; Aldous, L.; Hardacre, C.; Compton, R. G. *J. Phys. Chem. C* **2008**, *112*, 7725.
(18) Martinez-Huitle, C. A.; Brillas, E. *Angew. Chem., Int. Ed.* **2008**, *47*, 1998.
(19) Lowe, E. R.; Banks, C. E.; Compton, R. G. *Anal. Bioanal. Chem.* **2005**, *382*, 1169.
(20) Sun, G. Z.; Liu, S. W.; Hua, K. F.; Lv, X. Y.; Huang, L.; Wang, Y. J. *Electrochem. Commun.* **2007**, *9*, 2436.
(21) Mayell, J. S.; Langer, S. H. *Electrochim. Acta* **1964**, *9*, 1411.
(22) Dickinson, T.; Greef, R.; Wynne-Jones, L. *Electrochim. Acta* **1969**, *14*, 467.
(23) Sereno, L.; Macagno, V. A.; Giordano, M. C. *Electrochim. Acta* **1972**, *17*, 561.
(24) Rogers, E. I.; Streeter, I.; Aldous, L.; Hardacre, C.; Compton, R. G. *J. Phys. Chem. C* **2008**, *112*, 10976.
(25) Bonhote, P.; Dias, A. P.; Papageorgiou, N.; Kalyanasundaram, K.; Gratzel, M. *Inorg. Chem.* **1996**, *35*, 1168.
(26) MacFarlane, D. R.; Meakin, P.; Sun, J.; Amini, N.; Forsyth, M. *J. Phys. Chem. B* **1999**, *103*, 4164.
(27) Schroder, U.; Wadhawan, J. D.; Compton, R. G.; Marken, F.; Suarez, P. A. Z.; Consorti, C. S.; de Souza, R. F.; Dupont, J. *New J. Chem.* **2000**, *24*, 1009.
(28) Sharp, M. *Electrochim. Acta* **1983**, *28*, 301.
(29) Shoup, D.; Szabo, A. *J. Electroanal. Chem.* **1982**, *140*, 237.
(30) Bard, A. J.; Faulkner, L. R. *Electrochemical Methods, Fundamentals and Applications*, 2nd ed.; Wiley: New York, 2001.
(31) Gavaghan, D. J. *J. Electroanal. Chem.* **1998**, *456*, 1.
(32) Longhi, P.; Guerra, G. *Chim. Ind.* **1972**, *54*, 205.
(33) Mueller, L.; Kaiser, B. *Z. Phys. Chem.* **1980**, *261*, 1011.
(34) Hubbard, A. T. *Compr. Chem. Kinet.* **1989**, *28*, 20.

JP8082437